Neuron, Vol. 33, 95–106, March 28, 2002, Copyright ©2002 by Cell Press

Massive Light-Driven Translocation of Transducin between the Two Major Compartments of Rod Cells: A Novel Mechanism of Light Adaptation

Maxim Sokolov,[1,4] Arkady L. Lyubarsky,[2,4] Katherine J. Strissel,[1,4] Andrey B. Savchenko,[2] Viktor I. Govardovskii,[1,5] Edward N. Pugh, Jr.,[2] and Vadim Y. Arshavsky[1,3]
[1]Department of Ophthalmology
Harvard Medical School
Boston, Massachusetts 02114
[2]Department of Ophthalmology
School of Medicine
University of Pennsylvania
Philadelphia, Pennsylvania 19104

Summary

We report a new cellular mechanism of rod photoreceptor adaptation in vivo, which is triggered by daylight levels of illumination. The mechanism involves a massive light-dependent translocation of the photoreceptor-specific G protein, transducin, between the functional compartments of rods. To characterize the mechanism, we developed a novel technique that combines serial tangential cryodissection of the rat retina with Western blot analysis of protein distribution in the sections. Up to 90% of transducin translocates from rod outer segments to other cellular compartments on the time scale of tens of minutes. The reduction in the transducin content of the rod outer segments is accompanied by a corresponding reduction in the amplification of the rod photoresponse, allowing rods to operate in illumination up to 10-fold higher than would otherwise be possible.

Introduction

The vertebrate retina exhibits a remarkable ability to adapt to changes in the intensity of ambient illumination, allowing vision to function effectively over the more than ten orders of magnitude encountered during the normal diurnal cycle (Rodieck, 1998). Vision over this enormous range of intensities is partitioned between two photoreceptor types, rods and cones. A variety of molecular mechanisms have been discovered and quantified over the past two decades that enable both photoreceptor types to escape saturation as the illumination level increases and, thus, to function over a greater intensity range than would otherwise be possible (reviewed in Pugh, et al., 1999; Pugh and Lamb, 2000; Fain et al., 2001; Burns and Baylor, 2001; Arshavsky et al., 2002).

In the late 1980's and early 1990's, four groups reported that the α and β subunits of the photoreceptor-specific G protein, transducin, undergo light-dependent redistribution between rod outer segments and other photoreceptor compartments (Brann and Cohen, 1987; Philp et al., 1987; Whelan and McGinnis, 1988; Organisciak et al., 1991). More recently, Terakita et al. (1996; 1998) have found that both α and β subunits of G_q, which underlies phototransduction in invertebrate photoreceptors, also undergo light-dependent movement from the rhabdomere membranes to the photoreceptor cytoplasm. While it was hypothesized in these papers that such G protein redistribution might be generally adaptive, no evidence has been presented that in fact, it extends the range of light intensities over which photoreceptors operate. Moreover, the immunohistochemical data that support the redistribution of transducin were argued to be the result of an epitope-masking artifact (Roof and Heth, 1988), potentially undermining the very existence of the phenomenon in vertebrate rods.

The present study was undertaken to resolve the issue of whether transducin redistributes between the outer and inner segments of rods and, once resolved, to quantify the precise conditions of retinal illumination under which the redistribution occurs, as well as its time course, and finally, to determine if the redistribution is adaptive in the strict sense of extending the intensity range over which rods can function. To address these issues, we have developed a novel technique that combines serial tangential cryosectioning of the retina with Western blot analysis of the proteins in the serial sections. We applied this technique to analyze the distribution of transducin amongst the subcellular compartments of rods from rats exposed to illumination of various intensities and confirmed that light causes a massive light-dependent translocation of transducin between outer and inner segments of rods. We then showed that this movement is accompanied by a large change in the amplification of the rod photoresponse.

Results

We first replicated the immunohistochemical results (Brann and Cohen, 1987; Philp et al., 1987; Whelan and McGinnis, 1988) that were argued to support the case that transducin moves from the outer to the inner segment when dark-adapted rodents are exposed to strong illumination (Figure 1). However, Roof and Heth (1988) provided extensive evidence that such immunolocalization data may be compromised by an artifact based on light-dependent masking of the antibody-recognition epitopes on transducin. Roof and Heth also argued that there were artifacts in the quantification of proteins from isolated rod outer segments in experiments supporting the hypothesis of transducin movement (Philp et al., 1987; Whelan and McGinnis, 1988; Organisciak et al., 1991) due to incomplete preservation of their protein content or by contaminations from other cellular structures. Thus, we developed an alternative methodology not susceptible to most of these potential artifacts.

Western Blot Analysis of Serial Cryosections of Rat Retinas

The strategy developed to resolve the issue of transducin movement is explained in Figure 2. Retinas of

[3]Correspondence: vadim_arshavsky@meei.harvard.edu
[4]These authors contributed equally to this work.
[5]Present address: Institute of Evolutionary Physiology and Biochemistry, 44 Thorez Prospect, 194223 St. Petersburg, Russia.

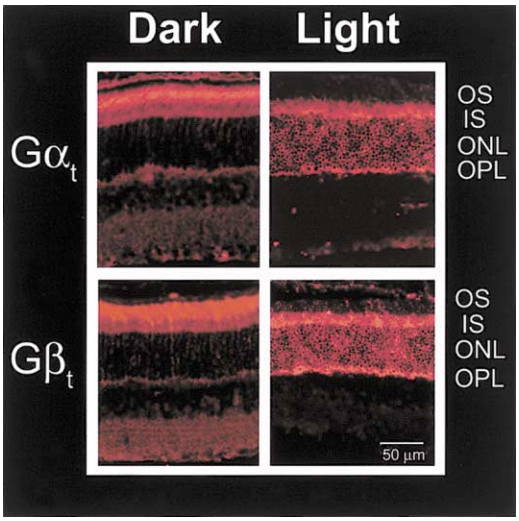

Figure 1. Immunohistochemical Detection of Transducin Localization in the Photoreceptors of Dark- and Light-Adapted Retinas

$G\alpha_t$ and $G\beta_t$ were detected in cross-sections of dark- or light-adapted rat retinas by immunofluorescence staining, as described in Experimental Procedures. Retinal layers are abbreviated as follows: OS, outer segment; IS, inner segment; ONL, outer nuclear layer; and OPL, outer plexiform layer.

dark- or light-adapted animals were rapidly extracted, flat mounted, and frozen without perturbing their morphology and then serially sectioned so that each section yielded one progressive tangential slice of the photoreceptor layer (Figure 2A). The protein content of each section was then analyzed by Western blotting, a technique not susceptible to the epitope-masking artifact. The serial cryosectioning methodology was originally developed for studying the distributions of small molecules such as cGMP throughout the retinal layers (Lolley and Farber, 1975; Orr et al., 1976; Govardovskii and Berman, 1981; de Azeredo et al., 1981; Blazynski and Cohen, 1986). Our contribution has been to adopt the serial cryosection technique for the investigation of protein distributions in the retina.

The spatial resolution of the technique is critical to its utility. It was assessed by analyzing the distribution of protein markers whose location within the photoreceptor cell is well-defined. Three markers were used (Figure 2B): (1) rhodopsin, located predominantly in the rod outer segment; (2) cytochrome C, confined to mitochondria, which are located in the ellipsoid region of the inner segment and the area near the synaptic terminus; and (3) synaptophysin, located in the presynaptic membrane vesicles. From comparison of the markers' distributions among the sections with the known morphology of rat rods (illustrated schematically in Figure 2C), it can be seen that the method provides a generally accurate representation of the subcellular location of these proteins in the rods. Some overlap of proteins confined to separate compartments results from imperfect alignment of the layers in the frozen tissue and also from minor misalignment of the sample with respect to the plane of the cryotome knife. Nonetheless, the degree of this overlap does not compromise protein assignments to specific rod compartments.

Light Causes Massive Translocation of Transducin from the Outer to the Inner Segments of Rods

The subcellular distribution of transducin in the rods of dark- and light-adapted rats found with the serial cryosection analysis is illustrated in Figure 3. In dark-adapted animals, the distribution of both α and β subunits of transducin ($G\alpha_t$ and $G\beta_t$, respectively) closely matches the distribution of rhodopsin, consistent with the localization in the outer segment seen in immunohistochemistry (Figure 1). In contrast, the distribution of the major fractions of both transducin subunits in light-adapted animals matches most closely the profile of cytochrome C in the inner segments, with only small fractions remaining in the rhodopsin-containing sections. These data establish that most transducin is redistributed from the rod outer segment into the inner segment and, to a lesser extent, into the rest of the rod cell body.

Densitometric analysis of the protein bands in Western blots was used to quantify the amount of transducin present in the rod outer segment under various conditions. We measured the density distributions (Figure 3) over the serial sections of four proteins: rhodopsin, cytochrome C, $G\alpha_t$, and $G\beta_t$; the latter was confirmed by co-immunoprecipitation to remain in a complex with the

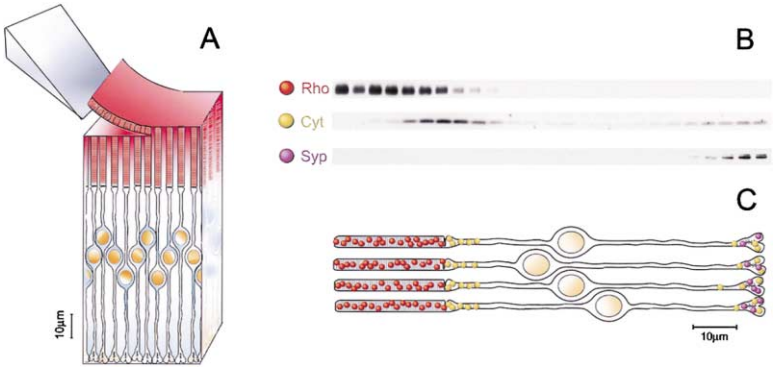

Figure 2. Determination of Protein Distribution throughout the Photoreceptor Layer of the Retina by Serial Tangential Cryosectioning with Western Blotting

(A) Schematic illustration of the principle of the serial tangential sectioning of the retina.

(B) Western blots showing distribution of three marker proteins of the photoreceptor cell compartments rhodopsin (Rho), cytochrome C (CytC), and synaptophysin (Syp). Each lane of the gel represents the protein content of a single 5 μm section into the retina starting from the outer segment tips and progressing inward.

(C) A drawing illustrating the distribution of these markers at their respective locations throughout the photoreceptor layer of the retina.

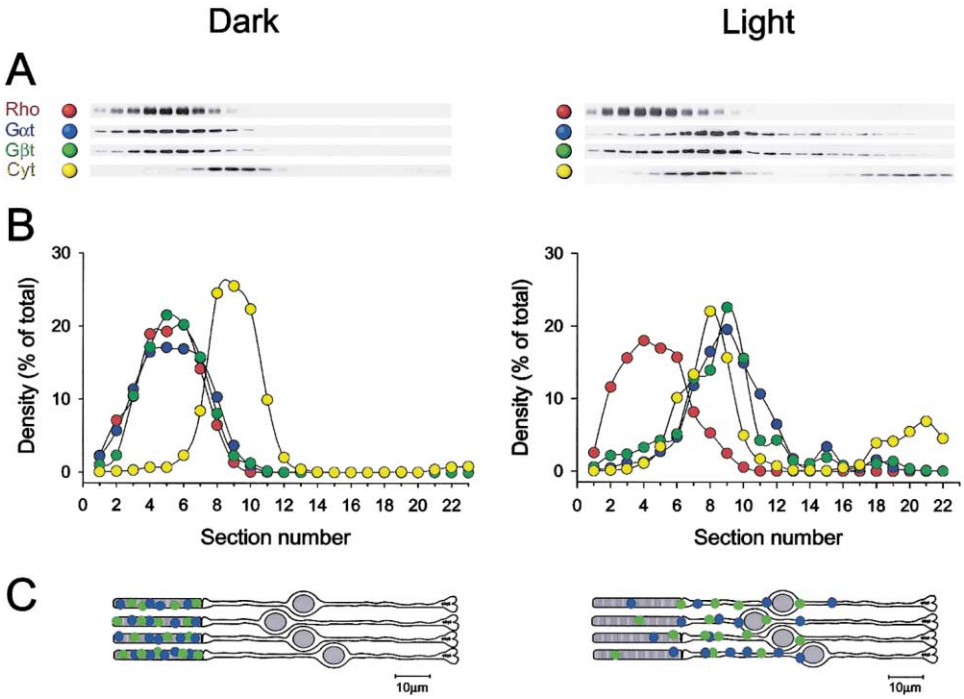

Figure 3. Quantitative Analysis of Transducin Content in Rod Compartments Using the Cryosectioning with Western Blotting Technique

(A) Western blots of $G\alpha_t$, $G\beta_t$, and two marker proteins in the serial sections obtained from the retinas of either a dark-adapted rat or a rat exposed to 1 hr illumination at a luminance of 240 scotopic cd m^{-2}.

(B) Densitometric profiles of the Western blots from (A). The densities of individual bands are expressed as a percent of the total density of all bands representing each individual protein on the blot.

(C) A drawing illustrating the distribution of $G\alpha_t$ and $G\beta_t$ at their respective locations throughout the photoreceptor layers of the dark- and light-adapted retinas.

transducin γ subunit in all experiments reported here. The density distributions over the retinal receptor layer were determined as follows. First, we identified those rhodopsin-containing sections that were free of inner segment contaminations, judged by the absence of cytochrome C (such as sections one through five in Figure 3A). We conducted further analysis only in the preparations where at least one of the two following conditions was met: either the number of rhodopsin-stained lanes that had no measurable cytochrome C staining was at least four, or the number of such lanes was three, but they contained at least one-half of the total rhodopsin content. Either of these criteria was met in about one of three retinas in which the analysis was attempted. Second, we determined the amounts of rhodopsin, $G\alpha_t$, and $G\beta_t$ present in the cytochrome-free sections as fractions of the total protein of each type present in all sections. Thus, in the data of Figure 3A, the cytochrome-free sections contained 58% of the total rhodopsin, 53% of the total $G\alpha_t$, and 52% of the total $G\beta_t$. Third, we derived the content of $G\alpha_t$ and $G\beta_t$ in the entire rod outer segment by dividing their percentage in the cytochrome C free sections by the percentage of rhodopsin in the same sections. So, for Figure 3A, the outer segment fraction of $G\alpha_t$ was 53%/58% = 0.91, or 91% of the total $G\alpha_t$ present in rods; the outer segment fraction of $G\beta_t$ was 52%/58% = 0.9. The $G\alpha_t$ content of the outer segments of the three completely dark-adapted animals was 86% ± 12% (mean ± SD; range 72%–96%) of the total. The $G\beta_t$ content in the outer segments of the same animals was 82% ± 10% (range 72%–91%). Percentages of $G\alpha_t$ and $G\beta_t$ in the dark-adapted outer segment lower than 100% could arise either because the amount of transducin at the tip of the outer segment is slightly lower than at the base or because a small fraction of transducin remains in the inner segment even after prolonged dark adaptation, as immunohistochemical data from Figure 1 suggest.

We applied the same analysis to the data of light-adapted rats and found a massive redistribution of transducin. Thus, for the rat of Figure 3B (light), the outer segments contained only 9% of the total $G\alpha_t$ and 20% of the total $G\beta_t$. The results presented in Figure 3 were obtained with anesthetized rats whose pupils were dilated, experimental conditions required to insure quantification and reliability. We confirmed that the effect is not restricted to these conditions using untreated animals exposed to daylight at the laboratory window (data not shown).

We next determined whether the transducin redistribution reflects the movement from the outer segment to other photoreceptor compartments or the degradation of the transducin in the outer segment combined with its rapid resynthesis in the inner segment. Results of two experiments revealed that movement alone underlies the redistribution. In the first experiment, the total amount of both transducin subunits in solubilized whole retinas, measured by quantitative Western blotting, re-

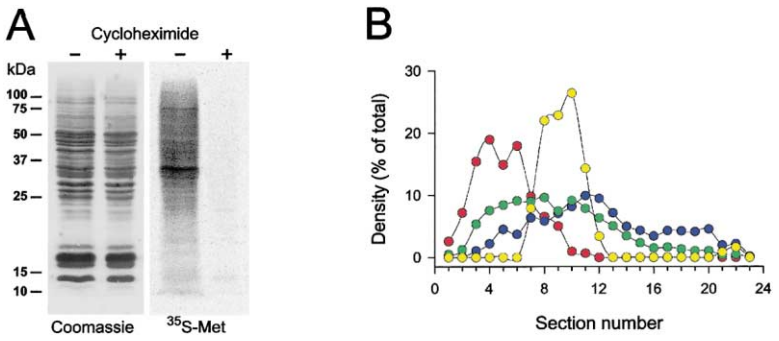

Figure 4. Suppression of Protein Synthesis in the Retina Does Not Preclude Transducin Translocation

Rats, either treated or untreated with cycloheximide, were subjected to 30 min of illumination at 460 scotopic cd m^{-2}.

(A) Retinas of one eye of untreated (−) or treated (+) animals were extracted and incubated with ^{35}S-methionine as described in the Experimental Procedures section. Homogenates of radiolabeled retinas were subjected to SDS-PAGE and transferred to PVDF membrane. The left image shows total protein staining on the blot, and the right image shows the corresponding ^{35}S incorporation on the same blot.

(B) The retina from the second eye of the treated animal was analyzed by serial tangential sectioning with Western blotting. The data are quantified and plotted as described in Figure 2B. The amount of $G\alpha_t$ translocation from the rod outer segments of the cycloheximide-treated animal was calculated to be ~83%, and of $G\beta_t$, ~68%. The data are taken from one of three similar experiments. Control experiments showed that cycloheximide did not affect transducin localization in the dark-adapted animals (data not shown).

mained unchanged in the course of transducin redistribution. The amount of $G\alpha_t$ measured in whole retinas after subjecting rats to the light conditions described for Figure 3 was 97% ± 19% of the dark content (SEM, n = 3; data not shown). The amount of $G\beta_t$ in the same animals was 99% ± 10% of the dark level. In the second experiment, a complete inhibition of protein synthesis in photoreceptors achieved by a systemic treatment with cycloheximide did not have a significant effect on the light-dependent transducin redistribution (Figure 4). The conservation of the total amount of both transducin subunits under varying conditions and the absence of an effect of cycloheximide reject the hypothesis that degradation and resynthesis account for the light-induced redistribution of protein.

The Light- and Time-Dependence of Transducin Translocation

The dependence of transducin movement on light intensity is illustrated in Figure 5A. Movement was detected after exposure to 1 hr illumination at intensities as low as 20 scotopic cd m^{-2}, estimated to isomerize rhodopsin at the initial rate of 2×10^4 R* rod^{-1} s^{-1} (where R* is photoexcited rhodopsin). This corresponds to excitation of about 0.02% of the rhodopsin content per s, assuming 10^8 rhodopsin molecules per rod outer segment. For $G\alpha_t$ translocation, the half-saturating light intensity was 40 scotopic cd m^{-2}, while half saturation of the movement of $G\beta_t$ occurred at 64 scotopic cd m^{-2}. At saturation, light caused translocation of ~90% of the rod outer segment $G\alpha_t$ and ~80% of $G\beta_t$.

The time course of transducin translocation was then investigated at a single light intensity (200 scotopic cd m^{-2}) adequate to saturate the movement of both $G\alpha_t$ and $G\beta_t$ in 1 hr exposures (Figure 5B). As suggested by the shift in light dependence in Figure 5A, $G\alpha_t$ was more mobile than $G\beta_t$, with a half-time to completion that is ~3-fold shorter (5 min for $G\alpha_t$ versus 12.5 min for $G\beta_t$). The time courses of the repopulation of the outer segment by $G\alpha_t$ and $G\beta_t$ at the extinction of the 1 hr light exposure were also investigated. The reappearance of the two subunits in the outer segment sections followed a very similar course with a half-time of 2.5 hr, much slower than their movement out of the outer segment.

The Amplification of Rod Phototransduction Decreases under Conditions that Cause Transducin Translocation

To assess whether the movement of transducin out of the rod outer segment has adaptive consequences for

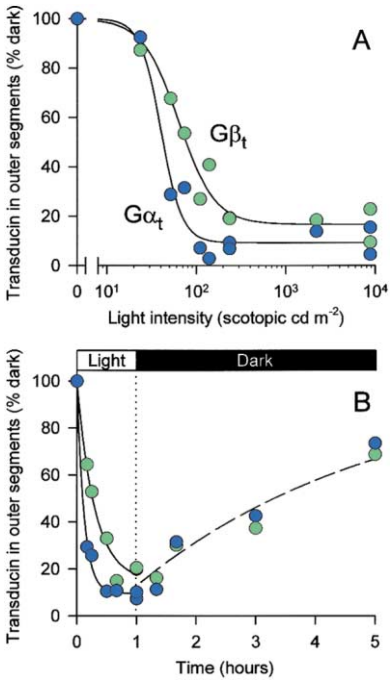

Figure 5. The Dependency of Transducin Translocation on the Intensity and Duration of Illumination

(A) The degree of $G\alpha_t$ and $G\beta_t$ translocation was determined after exposing rats for 1 hr to various light intensities. The data are fitted by the Hill equation, $y = y_o - a \times x^n/(x^n + b^n)$. For $G\alpha_t$: y_o = 100%, a = 91%, b = 40 scotopic cd m^{-2}, and n = 3.7. For $G\beta_t$: y_o = 100%, a = 83%, b = 64 scotopic cd m^{-2}, and n = 2.2.

(B) The time course of $G\alpha_t$ and $G\beta_t$ retranslocation after the onset of light having a luminance of 200 scotopic cd m^{-2}. Exponential curves fitted to the data and shown in the figure yielded the following rates: 90% of $G\alpha_t$ was redistributed from the rod outer segment layer at a rate of 0.14 min^{-1}; 85% of $G\beta_t$ was redistributed from the outer segments at 0.056 min^{-1}. The estimated rate of both subunits' return to the rod outer segments after the end of the illumination period was 0.004 min^{-1}.

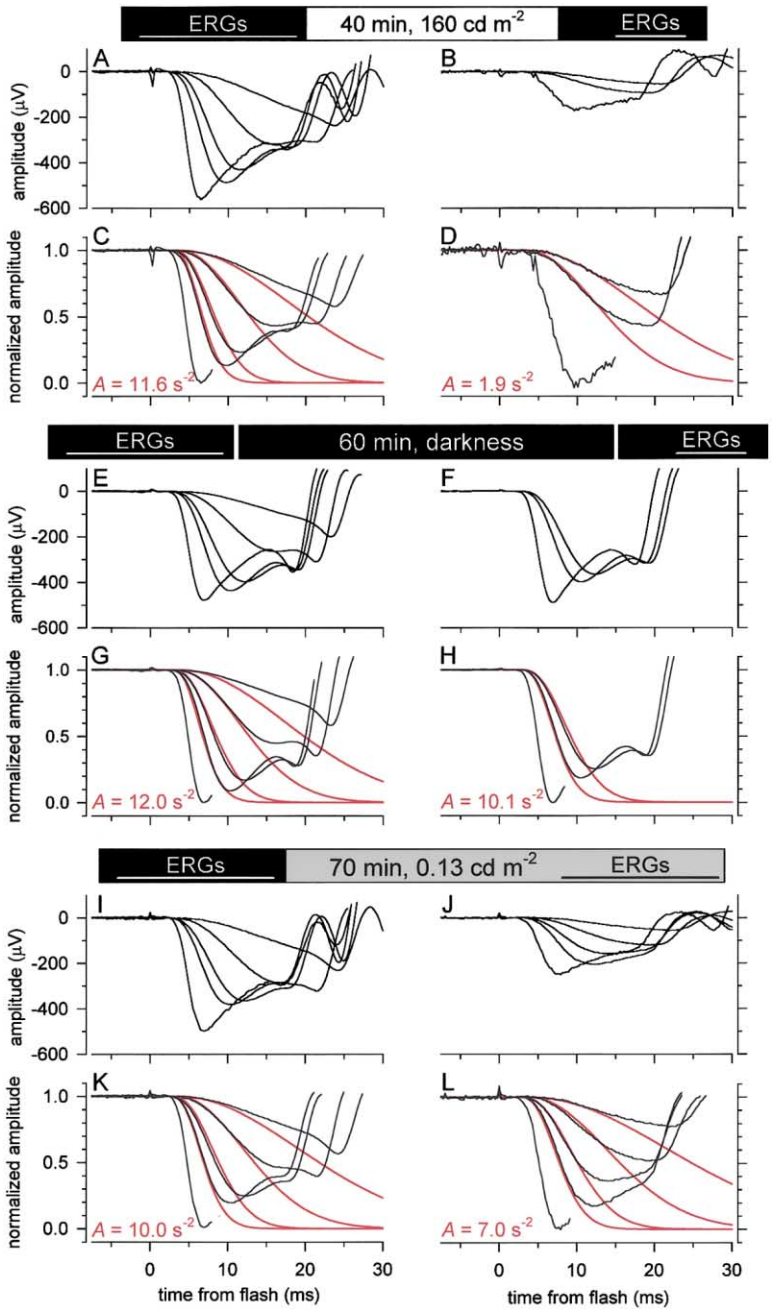

Figure 6. Estimation of the Amplification Constant of the Rod Transduction Cascade under Conditions that Produce Different Concentrations of Transducin in the Outer Segments

Each set of four panels presents ERG results from one rat, with the upper pair of panels in each set ([A and B], [E and F], and [I and J]) showing the raw records and the lower pair ([C and D], [E and F], and [K and L]) showing the corresponding traces normalized to the saturating a-wave amplitude. The experimental protocol used for each rat is illustrated by the bar above each four-panel set: black segments indicate times when the rat was in darkness, and the white segment (above [A] and [B]) and light-gray segment (above [I] and [J]) indicate periods when the rat was exposed to steady illumination. ERGs were measured at the times indicated by the lines and labels on the bars. Each ERG trace shown in (A), (B), (E), (F), (I), and (J) is the average of 15 individual responses from each eye (30 total records), with the exception of the response to the most intense flash, which is the average of one (B and F) or two responses from each eye (A, E, I, and J). In (C), (D), (G), (H), (K), and (L) the initial (a-wave) portions of the normalized traces have been fitted with theory curves to extract the amplification constant, *A*, (see Experimental Procedures) whose value is given in red. Each rat was sacrificed immediately after the last saturating flash and the eyes rapidly enucleated and placed in iced buffer for further analyses. One eye was processed for measurement of the unbleached rhodopsin fraction (see Experimental Procedures), which was used in calculating the number of photoisomerizations produced by each flash. The other eye was prepared for cryosectioning.

rod signaling, we measured the a-wave of the electroretinogram (ERG) under conditions identical to those used for characterizing the movement and further, completed a number of experiments in which ERGs and transducin movement were measured in the same animals. Panels A–D of Figure 6 were obtained from a rat exposed for 40 min to an intensity of 160 scotopic cd m^{-2}, established to produce maximal movement. (A) shows the family of ERGs collected in the dark-adapted state prior to onset of the steady adapting light and (B) shows ERGs collected beginning 15 min after the extinction of the adapting light. We used one saturating and four subsaturating flash intensities for the ERG family collected in the initial dark-adapted state (A), but only two of the four subsaturating flash intensities were used for the light-adapted ERG family (B) in order to keep the recording time after light offset to the minimum required for reliable analysis.

The a-wave of the rodent ERG is well established as a field potential originating almost exclusively in the suppression of rod circulating current (Hagins et al., 1970). To quantify the amplification of the rod photoresponse, we employed the model of the transduction cascade developed by Lamb and Pugh (1992) to analyze the responses of single rods and shown subsequently to apply to human and murine ERG a-waves (Lyubarsky and Pugh, 1996; Thomas and Lamb, 1999). The analysis requires that the a-waves be normalized to the saturating amplitude of the a-wave to provide a scale proportional to the normalized rod circulating current and, then, to be fitted with theoretical traces, as shown in Figures

Table 1. Summary of Effects of Illumination Intensity on the Amplification Constant and on Transducin Movement

Illumination Condition Intensity (scotopic cd m^{-2})	Symbol Used in Figure 7B	Number of Animals (n)	Saturated a-Wave Amplitude in Dark (μV)	Saturated a-Wave Amplitude at Termination (fraction of dark value)	Rhodopsin at Termination (fraction)	$\frac{A_{dark}}{A}$ (fold decrease)	$\frac{G_{t,dark}}{G_t}$ (fold decrease)
darkness	●	3	540 ± 55	0.85 ± 0.16	(1.0)	1.2 ± 0.1	1.2 ± 0.1 (n = 3) (1.1–1.3)
0.13	◍	3	530 ± 20	0.50 ± 0.03	1.03 ± 0.03	1.3 ± 0.2	1.3 (n = 1)
40	○	6	490 ± 90	0.60 ± 0.19	0.83 ± 0.06	2.3 ± 1.1	1.9 ± 1.1 (n = 2) (1.1–2.6)
65	◇	3	510 ± 130	0.33 ± 0.01	0.57 ± 0.06	4.6 ± 1.6	2.9 (n = 1)
110	▽	9	550 ± 90	0.34 ± 0.11	0.51 ± 0.10	4.7 ± 1.8	4.6 ± 1.6 (n = 4) (2.4–5.9)
160	□	11	500 ± 100	0.28 ± 0.11	0.58 ± 0.12	4.9 ± 1.8	9.4 ± 0.8 (n = 3) (8.4–10.1)

All data in the table were obtained from animals from which ERGs were measured; entries in columns 4 to 8 give the mean ± SD. For each animal, ERGs were first measured in the dark and then after an exposure condition given in column 1; the a-waves were analyzed as in Figure 6. Column 8 gives the fold reduction in the $G\alpha_t$ content of the rod outer segments obtained by dividing the average value from three fully dark-adapted animals (see text) by the value for animals exposed to the illumination condition of the row. The number of measurements in column 8 is given in parentheses after the error statistic; in addition, the range of the data is shown in parentheses on the second line. (Since only about 1/3 of retinas initially prepared for serial sectioning had an adequate number of the cytochrome-C free rhodopsin-staining sections to perform this quantification, the number of animals listed in column 8 of any row is less than that given in column 3 of the same row; however, each animal whose results are tabulated in column 8 also provided ERG data included in the other columns of the row.) The exposure condition lasted 60–70 min for all conditions, except for 9 (of 11 total) rats exposed to 160 cd m^{-2}; these 9 rats were exposed to the steady light for 40 min. This shortened duration exposure is responsible for the somewhat higher average fraction (0.58) of rhodopsin present in this group than might be expected from extrapolation of the data of animals exposed to lower intensities.

6C and 6D. A single constant, *A* (the "amplification constant"), governs the family of fitted traces and characterizes the combined contributions to amplification of the several steps of the transduction cascade. For the rat of Figures 6A–6D, $A = 11.6\ s^{-2}$ in the dark-adapted condition , while during the recovery period, $A = 1.9\ s^{-2}$, a 6.1-fold reduction. Similar experiments conducted with a total of 29 rats at four different illumination intensities are summarized in Table 1.

Two types of control experiments were performed to examine the possibility that the reduction in *A* was due to the lengthy exposure to anesthesia or to other aspects of the ERG protocol. In one set of control experiments, the animal was kept in darkness but received exactly the same set of test stimuli delivered at approximately the same times as animals in the experiments exposed to steady illumination; Figures 6E–6H illustrates one of these experiments. A slight decline in *A* was observed for these "dark controls" (Table 1); subsequent serial cryosection analysis revealed that the transducin levels in the outer segment layer were also slightly reduced (Table 1, column 8), most likely in response to the intense flashes needed to determine the saturating a-wave amplitude.

Another control experiment is illustrated in Figures 6I–6L. In this case, after measurement of the ERG response family in darkness, the rat was exposed to 70 min of dim illumination (0.13 scotopic cd m^{-2}) that suppressed about 50% of the rod circulating current. This intensity level was selected so that the saturating a-wave amplitude during the exposure was approximately the same as that measured during the recovery period of animals exposed to saturating levels of illumination (40–160 scotopic cd m^{-2}). During the last 20 min of illumination, ERGs were recorded in response to the same series of flashes as used to measure the dark-adapted response family. Analysis of these data showed that *A* declined only slightly (Figures 6K and 6L), again consistent with a small reduction in the rod outer segment transducin content (Table 1, column 8).

Figure 7 summarizes evidence supporting the identification of transducin translocation as the mechanism underlying the decrease in amplification. Figure 7A gives the average reduction in the amplification constant, obtained from the entire population of animals from which ERGs were collected, plotted as a function of the luminance of the exposure. Here, the amplification constant is expressed as a percentage of the value extracted initially, when the animal was fully dark adapted; analysis predicts (see Experimental Procedures) this percentage to be directly proportional to the percent of transducin present in the outer segment. Hence, for comparison, we have replotted from Figure 5A measurements of the $G\alpha_t$ content of the outer segment layer, along with the curve that was fitted to these data. The decrease in amplification occurs in the same intensity range as $G\alpha_t$ translocation, though there are discrepancies between the two sets of data at both ends of the light intensity scale. These discrepancies can be understood in terms of differences in the experiments used to make the two kinds of measurements. At the lower end of the scale, the data point plotted at zero represents animals in the dark control condition (Figure 6B). Unlike dark-adapted rats used only for the cryosection analysis, the animals in the ERG dark control group were exposed over the final 20 min of the experiment to three intense flashes, each of which isomerized 0.5% of their rhodopsin, and some $G\alpha_t$ movement was observed experimentally (Table 1). At the upper end of the intensity scale (points at 65, 110, and 160 cd m^{-2}), the discrepancy may arise because the ERGs were collected 15 to 25 min after the light exposure was terminated, allowing for some

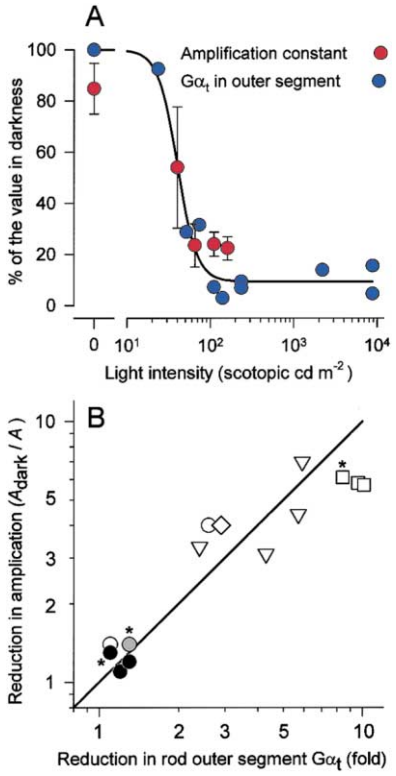

Figure 7. Evidence that Transducin Loss from the Outer Segment Underlies the Decline in Amplification

All results were obtained in one of the three experimental protocols illustrated in Figure 6.

(A) The amplification constant, expressed as a percentage of the value of the amplification constant in darkness, was measured after an exposure to steady illumination for 40–60 min and is plotted as a function of the illumination intensity (red circles); error bars are ± 2 SEM. The concentration of $G\alpha_t$ in the outer segment layer, relative to the concentration in darkness, is replotted from Figure 5A, along with the curve drawn through the data.

(B) Each point on the graph presents data of one rat whose ERGs were measured to determine the amplification constant in darkness and again after exposure to light or darkness (as in Figure 6) and for which the transducin content of the outer segment layer was also measured. The abscissa gives the reduction in the $G\alpha_t$ content in rod outer segments, referenced to the same ratio averaged from three completely dark-adapted rats. The ordinate gives the ratio of the amplification constant measured in the dark (A_{dark}) to that (A) measured after the exposure condition. Different symbols represent different illumination conditions, identified in Table 1. The data from the three animals whose ERGs are shown in Figure 6 are identified by asterisks.

repletion of the outer segment transducin level (cf. Figure 5).

Further evidence for the identification of transducin translocation as the mechanism underlying the change in amplification was obtained by correlating the reduction in amplification with the decrease in the outer segment $G\alpha_t$ content of individual rats. For example, for the rat of Figures 6A–6D, light caused a 6.1-fold reduction in A and an 8.3-fold reduction in outer segment $G\alpha_t$ content, whereas for the rat of Figure 6I–6L, light caused a 1.4-fold reduction in A and a 1.3-fold reduction in $G\alpha_t$. In Figure 7B, we plot this comparison for all rats used in the ERG experiments for which we also had successful serial cryosection analyses. The abscissa of this graph is the "fold" reduction in $G\alpha_t$ content in the outer segments. The ordinate of the graph is the fold reduction in the amplification constant (A); that is, A_{dark}/A where A_{dark} is the constant calculated from the a-wave response family obtained in the dark adapted state, and A is the value calculated from the a-wave family measured at the end of the experimental manipulations. The symbols in the graph identify the different experimental conditions (see Table 1 for symbol legend). Also presented in this double-log plot is a unity slope line, which represents the prediction that the amplification constant should scale in direct proportion to the transducin content of the rod outer segment (see Equation 5 in Experimental Procedures).

Discussion

The central result of the present investigation is that transducin undergoes a massive light-dependent redistribution in the rods of living animals. While consistent with the conclusion of previous immunohistochemical studies, the result now rests firmly on a novel experimental technique that combines serial tangential cryosectioning of flat-mounted retina with protein analysis in the section by Western blotting. It bears emphasis that the technique of serial tangential sectioning with Western blotting can be used for the quantification of the cellular and subcellular distribution of any protein in the retina. Furthermore, the technique should be applicable to the investigation of protein distributions in other layered tissues, such as cerebral cortex.

The Rate of Transducin Activation by R* Is Directly Proportional to Transducin Concentration In Vivo

Our results support the hypothesis that the rate of transducin activation by R* in vivo is directly proportional to the concentration of transducin in the outer segment (Figure 7B). That such proportionality should occur is predicted by the findings of Heck and Hofmann (2001). These authors reconstituted bovine rod membranes stripped of their endogenous transducin with purified transducin (G_t) and measured the dependence of the rate of G_t activation per R* on the surface density of G_t. At mammalian body temperature, the K_m for this reaction was estimated to exceed 3,000 molecules of G_t per μm^2 of membrane, whereas the actual density is ~2,000 G_t molecules per μm^{-2} (calculated from the G_t: rhodopsin ratio of 1/12 in murine rods from Tsang et al. [1998] and a rhodopsin density of ~25,000 molecules per μm^{-2}.) The observed nearly linear dependence of the amplification constant on G_t (Figure 7B) thus follows as a consequence of the hypothesis that transducin activation in vivo follows a Michaelis dependence on G_t concentration combined with the observation that this concentration is always less than the K_m. This conclusion is also consistent with our recent observation that the rate of G_t activation per R* measured in disrupted rod outer segments under optimized conditions (Leskov et al., 2000) is several fold lower than the rate observed at saturating G_t concentrations (Heck and Hofmann, 2001).

Transducin Translocation Is a Novel Mechanism of Light Adaptation in Mammalian Rods

Our results provide strong support for the hypothesis that transducin translocation from the outer segment serves as a mechanism of rod light adaptation, allowing rodent rods to operate in the presence of higher illumination levels than would otherwise be possible.

Light adaptation, in its most general sense, comprises all changes in photoreceptors that occur as a consequence of increasing steady illumination. One hypothesized adaptational mechanism is a light dependent reduction in the rate at which R* activates transducin. Several investigators have concluded that there is a reduction in R* gain under some conditions (Lagnado and Baylor, 1994; Jones, 1995; Gray-Keller and Detwiler, 1996), although no reduction was observed by others (Hood and Birch, 1993; Thomas and Lamb, 1999; Nikonov et al., 2000). The most recent of these studies (Nikonov et al., 2000) found that the reactions that mediate photoresponse inactivation and recovery cause deviation of the response from its initial trajectory at much earlier times than previously thought (less than 100 ms for moderate intensity backgrounds at room temperature), making it essential to restrict analysis of R* gain to the earliest region of the rising phase of the response. Analysis of the fractional response at these very early times showed the initial rise of the response to be invariant with adaptational state for backgrounds suppressing up to 75% of the circulating current and applied for periods of several minutes. Thus, under these *subsaturating* illumination conditions, there was no evidence of significant reduction in the amplification constant. Our ERG a-wave data confirm this observation, showing very little change in the amplification of the rat rod photoresponse during exposure to illumination suppressing up to 2/3 of the rod circulating current for a full hour (Figures 6I–6L; Table 1). Similar results in experiments utilizing ERG a-waves to measure the human rod photocurrent in the presence of subsaturating backgrounds have been previously reported (Hood and Birch, 1993; Thomas and Lamb, 1999).

To the contrary, when rat rods are exposed in vivo to a strongly *saturating* background light that triggers transducin translocation, the amplification of the signaling cascade is subsequently reduced 5-fold or more (Figures 6C and 6D, Figure 7, Table 1). Consistent with these observations, Kennedy et al. (2001) have recently reported a long-lasting decrease in amplification in mice recovering from a flash that bleached 20% of their rhodopsin. The most parsimonious explanation of the decrease in amplification during recovery from exposure to strongly saturating backgrounds is that loss of transducin from the outer segment decreases the rate at which each newly formed R* activates transducin. Thus, the experiments reported here reveal specific conditions under which R* gain reduction indeed takes place.

Transducin translocation to the inner segment appears to underlie another somewhat surprising observation made in our study, the ability of rat rods to signal electrically with a substantial fraction of their rhodopsin in the bleached state. Under the conditions of experiments, such as that of Figures 6A–6D, when steady-state rhodopsin bleaching has reached about 50%, it takes rods less than 10 min after extinction of the steady light to recover 30% of their circulating current (Figure 6B; Table 1, columns 5 and 6). We hypothesize that transducin translocation contributes significantly to this ability of rodent rods to escape saturation and function electrically with such large fractions of unregenerated rhodopsin. Many studies have shown that decay intermediates of R*, collectively identifiable as unregenerated rhodopsin, create a kind of "dark light," causing substantial activation of the transduction cascade (reviewed by Leibrock et al., 1998; Fain et al., 1996). Transducin translocation would reduce this dark light, provided that the decrease in outer segment G_t concentration not only diminishes the gain of any newly formed R*s (as our experiments show), but also proportionately decreases the activity of all decay intermediates of R* present. This latter assumption is reasonable, providing the affinity of the decay intermediates for G_t is no greater than that of R* itself for G_t.

By reducing the gain of R* and its decay intermediates, transducin translocation will permit the rat rod to function in the presence of steady light intensities significantly higher than otherwise possible. Thus, when amplification has been decreased by 5-fold, rods will be able to function electrically in the presence of 5-fold higher steady light intensities. A still further extension of the operating range will be contributed by the reduced concentration of rhodopsin. In many of our experiments, a-wave responses were measured from rods having 50% or more of their rhodopsin in the bleached state. Such "pigment depletion" will cause a proportionate decrease in ability of rods to capture light. Thus, combining a 5-fold decrease in amplification with a 2-fold effect of rhodopsin depletion, the laboratory conditions that produce the large-scale transducin translocation, causes an overall 10-fold extension of the upper end of the intensity range in which rods can function without being driven into saturation. The effect of transducin translocation, per se, appears limited to a 10-fold decrease since $G\alpha_t$ loss from the outer segment does not exceed 90% at any light intensities (Figure 5). This limitation might serve to insure that the rod remains in saturation during its exposure to bright light and that some signaling capacity is available as soon as the rod comes out of saturation.

Could transducin translocation be an effective mechanism of adaptation under natural conditions? The light intensities that cause transducin translocation are saturating for rods so that vision under such conditions is governed by cones. Nonetheless, the reduction of transducin in rod outer segments will make it possible for rat rods to recover their ability to signal more rapidly after a strong light is extinguished or dimmed and, thus, to function in higher intensities than otherwise possible. Given the diurnal cycle under which animals in the wild live, it can be speculated that a rodent might avail itself of this expansion of the operating range of rod function after an episode when it is foraging with its cone vision and returns to its burrow or, perhaps, as dusk approaches. We stress that the light intensities causing transducin movement are likely to be encountered in ordinary daylight. Using the same light meter employed to calibrate the intensities used in our experiments, we found that the walls in our laboratories, illuminated by fluorescent lights, have luminances close to 1000 scotopic cd m^{-2} and that in external daylight, secondary

sources, including the sky, readily reach several thousand scotopic cd m^{-2}. Thus, even with fully constricted pupils, which in pigmented rodents reduce the retinal illuminance about 20-fold (Pennesi et al., 1998), modest duration exposures to daylight conditions will cause maximal transducin translocation, as we have observed in experiments with rats exposed to daylight near laboratory windows.

Hypotheses about the Mechanisms Underlying Transducin Movement

The principal challenge for future studies is the elucidation of the cellular and molecular mechanisms underlying transducin movement. Of critical importance will be experiments that distinguish movement governed by cytoplasmic diffusion from movement involving molecular motors. $G\alpha_t$ has long been known to become soluble upon transducin activation by R* (reviewed by Arshavsky et al., 2002), and the hypothesis that loss of $G\alpha_t$ from the rod outer segment is effected by cytoplasmic diffusion remains viable. In this case, transit through the outer segment largely occupied by the photoreceptor discs and through the narrow ($\sim$0.15 μm diameter) cilium joining the outer and inner segments would likely be rate limiting. Moreover, the concentration profile of $G\alpha_t$ after strong light exposure (Figure 4B) suggests that a diffusion account of the data will need to include strong binding in the inner segment since the cytoplasmic volume of the latter is only 2- to 3-fold greater than that of the outer segment, while after maximal distribution, the $G\alpha_t$ content of these two segments differs by up to 10-fold. The delayed loss of $G\beta\gamma_t$ from the outer segment and its relatively slower redistribution to the inner segment (Figure 5B) suggests that additional factors other than those that govern the movement of $G\alpha_t$ are at play. It bears note that $G\beta\gamma_t$ is fairly lipophilic and not readily solubilized from outer segment membranes in isotonic buffers (Kuhn, 1981). Finally, the facts that transducin returns to the outer segment during dark adaptation far more slowly than it exits and that both transducin subunits appear to return on the same time course (Figure 5B) suggest that their return to the outer segment may not be governed by the same mechanisms as their loss and that strong binding partners may be present in the inner segment for either or both subunits.

Most of the previous work on protein trafficking between the rod inner and outer segments has been devoted to the investigation of the delivery of newly synthesized proteins to the outer segment (see Tai et al., 1999; Marszalek et al., 2000; and Tam et al., 2000, for recent updates); in such investigations, the rod has served as a model system for investigating "vectorial" trafficking of protein constituents to a specific functional compartment of cell, the outer segment. Our investigation reveals that the rate of movement of transducin out of the outer segment can exceed that of newly synthesized protein into the outer segment by over 100-fold, and, thus, it will be particularly interesting to determine how these different movements co-exist, especially in the narrow rod cilium. The rod, which has long been a fruitful model for the investigation of G protein signaling, may now serve as a convenient model system for the study of signal-dependent protein redistribution in neurons.

Experimental Procedures

Animals

Experiments were carried out with 75–125 g female Long Evans rats. Animals were dark adapted for at least 12 hr prior to all experiments and anesthetized by intraperitoneal injection of a ketamine/xylazine mixture (75/20 mg/kg, respectively). In experiments involving light exposure, the animals' pupils were dilated with 1% cyclopentolate-HCl, 2.5% phenylephrine, 0.25% tropicamide. At the end of each experiment, anesthetized animals were sacrificed by cervical dislocation.

Steady Light Stimulation, Measurement, and Conversion to Rhodopsin Isomerization Rates

In biochemical and histological experiments conducted in Boston, light was delivered to each eye separately by a bifurcated fiber optic guide connected to an adjustable light source equipped with a 100 W halogen bulb. To achieve even illumination throughout the entire retina, a white semitransparent screen was positioned between the eye and the light source. The light intensity on the eye surface was measured with a calibrated photodiode attached to a PDA-700 amplifier (TTI Inc., Oriskany, NY). The photodiode head was equipped with an SSC filter that closely approximated a rat rhodopsin absorption spectrum; thus, all light incident on the diode was converted to rhodopsin-equivalent units. Using standard formulas (Wyszecki and Stiles, 1982) and taking into consideration the effective aperture of the diode casing, the equivalent luminance of a hemispheric surface ("ganzfeld") encasing the rat eye was derived. Thus, such a surface, having a luminance of 1 scotopic cd m^{-2} illuminating the diode placed at its center, would generate a flux density of 4.7×10^3 photons (500 nm) s^{-1} μm^{-2} at the diode surface.

For ERG experiments in Philadelphia, rats were placed in a Faraday cage that also served as a ganzfeld. For calibration of the steady illumination, a photodiode and amplifier identical to those used in Boston was employed. To convert illumination into estimated rates of photoisomerization, we used a formulation developed for mice (Lyubarsky and Pugh, 1996; Lyubarsky et al., 1999), making the assumption that the rat eye is congruent in form. Accordingly, a ganzfeld having a luminance of 1 scotopic cd m^{-2} is estimated to produce a photoisomerization rate in rat rods of $\sim 10^3$ s^{-1}.

Serial Tangential Sectioning with Western Blotting

Eyes were enucleated and dissected under dim red light. Retinas were placed in ice-cold Ringer's solution (130 mM NaCl, 3.6 mM KCl, 2.4 mM $MgCl_2$, 1.2 mM $CaCl_2$, 0.02 mM EDTA, 10 mM HEPES-NaOH (pH 7.4) adjusted to 313 mosM). Retinas were flat mounted by placing them between two glass slides separated by 0.5 mm spacers. This "sandwich" was then clamped with two small binder clips and immediately frozen on dry ice. The bottom slide of the sandwich, which contacts the basal membrane of the retina, was roughened by sandpaper to insure adhesion. The top slide facing the photoreceptors was covered with polytetrafluoroethylene spray to facilitate its subsequent separation from the retina. For sectioning, the clips were removed, the glass slides separated, and the bottom slide with the attached retina was mounted on the cryomicrotome specimen holder. The retina was trimmed to remove any folded edges and sequential 5 μm tangential retinal sections were obtained using a Microm HM 500 OM cryomicrotome. Each section was collected in 100 μl of SDS-PAGE sample buffer. Aliquots from each sample were subjected to SDS-PAGE followed by Western blotting. Proteins of interest were probed with specific antibodies and visualized by ECL (Amersham Pharmacia Biotech). The 4A antibody against $G\alpha_t$ was a gift from Dr. H.E. Hamm (Vanderbilt University), $G\beta_t$ (against the KTREGNVRVS peptide) was a gift from Dr. W.F. Simonds (NIH), and rhodopsin (4D2) was a gift from Dr. R.S. Molday (University of British Columbia). Anti-cytochrome C (H-104) and anti-synaptophysin (SVP38) antibodies were from Santa Cruz Biotechnology. Band densities were quantified on the Personal Densitometer SI (Molecular Dynamics) using ImageQuant software.

Protein Biosynthesis Inhibition

Two intraperitoneal injections of cycloheximide at 25 mg/kg were delivered to dark-adapted rats at a 1 hr interval. 1 hr after the second

injection, rats were subjected to illumination causing a maximal protein translocation. The retina from one eye was analyzed by serial tangential cryosectioning with Western blotting to determine the extent of transducin transoclation. The second eye provided a probe for determining the degree of protein biosynthesis inhibition, assessed by the degree of ^{35}S-methionine incorporation into the retinal proteins as follows. The retina was extracted and incubated in 0.5 ml of Ringer's solution containing 20 mM glucose and 20 μCi of ^{35}S-methionine for 30 min at room temperature. The retinas were then washed three times with 1.0 ml Ringer's solution and dissolved in 0.2 ml of SDS-PAGE sample buffer. Proteins were separated by SDS-PAGE and transferred to PVDF membrane. Total proteins were visualized by Coomassie R250 staining of the PVDF membranes, and ^{35}S-labeled proteins were detected on the same membranes using the Storm 860 Phosphoimagerystem (Molecular Dynamics).

Immunohistochemistry

Our procedure was similar to that described by Philp et al. (1987) with the following changes. Dissected rat eyecups were fixed in 4% formaldehyde (pH 7.5) for 1.5 hr at 20°C and incubated overnight in Tissue Freezing Compound (Fisher Scientific). Eyecups were frozen and 8 μm ocular cross-sections were cut and collected. For immunostaining, sections were air-dried for 30 min, rehydrated in PBS, and incubated in PBS containing 0.1% Triton X-100 for 15 min. After washing, sections were incubated 1 hr with 3% normal goat serum and incubated ~14 hr with the 4A antibody for $G\alpha_t$ or the C-16 antibody for $G\beta_t$ or control antibodies, followed by anti-mouse or anti-rabbit fluorescent Cy3-conjugated secondary antibodies (Jackson Immunochemicals).

Rhodopsin Measurements

Rhodopsin content in homogenized retinas was determined by difference spectroscopy before and after complete bleaching of the sample using the molar extinction coefficient of 40,500. The degree of rhodopsin bleaching in the retina was determined from the ratio of rhodopsin concentrations in aliquots of homogenized retina before and after regeneration with 11-cis-retinal, as follows. A retina, dissected in iced PBS under infrared illumination from the excised eye was osmotically shocked in 1 ml distilled water and vortexed for 2 min. The suspension was then filtered through a 70 μm nylon filter (Falcon) and the filtrate sonicated by ten 5 s pulses from a Sonics VC130PB sonicator. Four 450 μl aliquots were collected: 4.5 μl of 2.2 mM 11-cis-retinal was added to two of the aliquots, sonication was repeated, and regeneration conducted for 40 min at 37°C. The rhodopsin concentration was then measured by difference spectroscopy after addition of 5 μl 1 M hydroxylamine to each of the four aliquots.

Electroretinographic Measurements

ERGs were recorded simultaneously from both eyes using published methods (Lyubarsky et al., 1999). In brief, ERGs were recorded from anesthetized rats in a ganzfeld that also served as a Faraday cage, with differential amplifiers having bandwidth 0.1 Hz to 1 KHz; analog records were sampled and digitized at 5 KHz and stored for subsequent analysis. The corneal electrodes were platinum wires embedded in small plastic armatures terminating in hemispherical contact lenses; electrical contact was made with Goniosol (CIBAVision Ophthalmics), which also served to protect the cornea. The reference electrode was a tungsten needle inserted subcutaneously in the forehead. Pupils were dilated with 1% Mydriacil (Alcon). Goniosol and Mydriacil were re-administered after approximately 1 hr. Pupil size was measured at the beginning and the end of the recording periods and was found to be unchanged.

Flash Stimulation and Calibrations

The methods used for flash stimulation and calibration of flash stimuli have been given in detail in (Lyubarsky et al., 1999). In brief, monochromatic (510 nm) flash stimuli were calibrated in terms of photons μm^{-2} *at the cornea* and converted to estimated numbers of isomerizations per rod (Φ). Two flash series were used to produce ERG a-waves from which we estimated the amplification constant. Each series contained 31 flashes, incorporating 15 repetitions of each of two flashes of different intensities that did not saturate the a-wave amplitude, terminated by an intense flash that produced a saturated a-wave amplitude. Thus, expressed in photoisomerizations (Φ), *Series a* delivered 31 flashes producing Φ = [450 (15×), 1400 (15×), 500,000 (1×)] photoisomerizations, while *Series b* delivered Φ = [5100 (15×), 13,000 (15×), 500,000 (1×)]. Each series required approximately 10 min to complete. At least 5 min was allowed between presentations of the most intense flash, and the interflash intervals in the other cases were established in preliminary experiments to be sufficient for complete recovery of the responses between successive presentations under dark-adapted conditions. When ERGs were measured in dark-adapted or steady-state conditions, both *Series a* and *Series b* were used. During the initial 10–20 min of recovery from a 1 hr light exposure, the intense saturating flash was delivered at 5 min intervals to assess the saturating amplitude of the a-wave; when this achieved approximately 30% of the magnitude obtained in the initial, dark-adapted condition, *Series b* was applied and the rat was sacrificed immediately thereafter.

Theoretical Analysis of ERG a-Waves to Extract the Amplification Constant

To quantify the amplification of rod phototransduction we employed the model of the cascade developed by Lamb and Pugh (1992) to analyze the responses of single rods, and shown subsequently to apply to ERG a-waves. This model predicts the following relation:

$$1 - \frac{a(t)}{a_{max}} = F(t) = \exp[-\tfrac{1}{2}\Phi\, A(t - t_{eff})^2] \quad (1)$$

Here, $a(t)$ is the corneal-negative ERG a-wave; a_{max}, the saturating amplitude; $F(t)$, the fractional cGMP-activated current of the rods; Φ, the flash intensity given in photoisomerizations rod^{-1}; A, the amplification constant; and t_{eff}, a brief delay. For simplicity, we will call the expression on the left hand side of Equation 1 the "normalized a-wave" or "normalized amplitude," since it scales raw a-wave traces so that they range between unity in the dark and zero after saturating stimulation.

To fit the cascade model to rat a-waves, we used the modified version of Equation 1 which was developed by Smith and Lamb (1997) and incorporated the membrane time constant fixed at 1.3 ms. With this modification, we fitted Equation 1 to a-wave families using the "ensemble fitting" method, varying t_{eff} and A to obtain the best fit by eye to the a-wave family. For the 75 a-wave response families obtained from 36 rats and so fitted, t_{eff} was invariably found to lie between 1 and 2 ms.

In fitting Equation 1 to the a-waves, we took explicit account of the fact that under some of the conditions, substantial amounts of rhodopsin was in the bleached form and, hence, unable to capture light and initiate transduction. Thus, after the last series of ERGs was measured, each animal was rapidly sacrificed, and its eyes enucleated and put into iced PBS, a process that took less than 5 min. One retina was used to determine the fractions of bleached and unbleached rhodopsin, as described above; the second was used for the analysis of transducin distribution by cryosectioning with Western blotting. The flash intensities were then adjusted for the rhodopsin content; hence, if a flash was estimated to produce Φ photoisomerizations rod^{-1} in a dark-adapted animal, the same flash was taken to produce (1-B) × Φ photoisomerizations rod^{-1} when delivered to an animal that had a fraction B of its rhodopsin bleached at the time of the final a-wave measurements.

Prediction of the Relationship between the Amplification Constant and the Transducin Concentration of the Rod Outer Segment

The relationship between the amplification constant, A, and the concentration of G_t in the outer segment can be predicted as follows. First, A is expressible as the product of rate parameters from each of the successive stages of the cascade contributing to its overall amplification (Lamb and Pugh, 1992):

$$A = \nu_G\, c_{GE} \beta_{sub}\, n_{cG}, \quad (2)$$

where ν_G is the rate with which an R* activates transducin, c_{GE} is the coupling efficiency between activated transducin and phospho-

diesterase, β_{sub} is the rate constant of a single activated phosphodiesterase catalytic subunit, and n_{cG} is the Hill coefficient of the cGMP-activated channels. Second, Heck and Hoffman (2001) found ν_G to obey a Michaelis relation with respect to the membrane-bound transducin:

$$\nu_G = \nu_{G,max} \frac{G_t}{G_t + K_m}. \quad (3)$$

Here, $\nu_{G,max}$ is the saturating rate of activation, G_t is the surface density of transducin on the disc membranes, and K_m is the surface density yielding a half-maximal rate. At body temperature, the K_m exceeds the actual surface density of G_t in mammalian rods (see Discussion). It follows that in rat rods under the conditions of our experiments, Equation 3 should apply as:

$$\nu_G \approx \nu_{G,max} \frac{G_t}{K_m}. \quad (4)$$

Combining Equations 2 and 4, we arrive at the prediction:

$$\frac{A}{A_{dark}} = \frac{G_t}{G_{t,dark}}, \quad (5)$$

where A_{dark} is the amplification constant under fully dark-adapted conditions, A is the value in any condition when the transducin density in the disc membranes is expected to be altered, G_t is the concentration of transducin, and $G_{t,dark}$ is the concentration in the dark-adapted state.

Acknowledgments

This work was supported by NIH grants EY-10336 to V.Y.A. and EY-02660 to E.N.P., U.S. Civilian Research and Development Foundation grant RB1-217 to V.I.G. and V.Y.A., Massachusetts Lions Eye Research Fund to V.Y.A., and Knights Templar Award to K.J.S.; V.Y.A. and E.N.P. are recipients of Jules and Doris Stein Professorships from Research to Prevent Blindness, Inc.

Received: October 23, 2001
Revised: February 6, 2002

References

Arshavsky, V.Y., Lamb, T.D., and Pugh, E.N., Jr. (2002). G proteins and phototransduction. Annu. Rev. Physiol. *64*, 153–187.

Blazynski, C., and Cohen, A.I. (1986). Rapid declines in cyclic GMP of rod outer segments of intact frog photoreceptors after illumination. J. Biol. Chem. *261*, 14142–14147.

Brann, M.R., and Cohen, L.V. (1987). Diurnal expression of transducin mRNA and translocation of transducin in rods of rat retina. Science *235*, 585–587.

Burns, M.E., and Baylor, D.A. (2001). Activation, deactivation, and adaptation in vertebrate photoreceptor cells. Annu. Rev. Neurosci. *24*, 779–805.

de Azeredo, F.A., Lust, W.D., and Passonneau, J.V. (1981). Light-induced changes in energy metabolites, guanine nucleotides, and guanylate cyclase within frog retinal layers. J. Biol. Chem. *256*, 2731–2735.

Fain, G.L., Matthews, H.R., and Cornwall, M.C. (1996). Dark adaptation in vertebrate photoreceptors. Trends Neurosci. *19*, 502–507.

Fain, G.L., Matthews, H.R., Cornwall, M.C., and Koutalos, Y. (2001). Adaptation in vertebrate photoreceptors. Physiol. Rev. *81*, 117–151.

Govardovskii, V.I., and Berman, A.L. (1981). Light-induced changes of cGMP content in frog retinal rod outer segments measured with rapid freezing and microdissection. Biophys. Struct. Mech. *7*, 125–130.

Gray-Keller, M.P., and Detwiler, P.B. (1996). Ca^{2+} dependence of dark- and light-adapted flash responses in rod photoreceptors. Neuron *17*, 323–331.

Hagins, W.A., Penn, R.D., and Yoshikami, S. (1970). Dark current and photocurrent in retinal rods. Biophys. J. *10*, 380–412.

Heck, M., and Hofmann, K.P. (2001). Maximal rate and nucleotide dependence of rhodopsin-catalyzed transducin activation: initial rate analysis based on a double displacement mechanism. J. Biol. Chem. *276*, 10000–10009.

Hood, D.C., and Birch, D.G. (1993). Light adaptation of human rod receptors: the leading edge of the human *a*-wave and models of rod receptor activity. Vision Res. *33*, 1605–1618.

Jones, G.J. (1995). Light adaptation and the rising phase of the flash photocurrent of salamander retinal rods. J. Physiol. (Lond.) *487*, 441–451.

Kennedy, M.J., Lee, K.A., Niemi, G.A., Craven, K.B., Garwin, G.G., Saari, J.C., and Hurley, J.B. (2001). Multiple phosphorylation of rhodopsin and the in vivo chemistry underlying rod photoreceptor dark adaptation. Neuron *31*, 87–101.

Kuhn, H. (1981). Interactions of rod cell proteins with the disc membrane: influence of light, ionic strength, and nucleotides. Curr. Top. Membr. Transp. *15*, 171–201.

Lagnado, L., and Baylor, D.A. (1994). Calcium controls light-triggered formation of catalytically active rhodopsin. Nature *367*, 273–277.

Lamb, T.D., and Pugh, E.N., Jr. (1992). A quantitative account of the activation steps involved in phototransduction in amphibian photoreceptors. J. Physiol. (Lond.) *449*, 719–758.

Leskov, I.B., Klenchin, V.A., Handy, J.W., Whitlock, G.G., Govardovskii, V.I., Bownds, M.D., Lamb, T.D., Pugh, E.N., Jr., and Arshavsky, V.Y. (2000). The gain of rod phototransduction: reconciliation of biochemical and electrophysiological measurements. Neuron *27*, 525–537.

Leibrock, C.S., Reuter, T., and Lamb, T.D. (1998). Molecular basis of dark adaptation in rod photoreceptors. Eye *12*, 511–520.

Lolley, R.N., and Farber, D.B. (1975). Cyclic nucleotide phosphodiesterases in dystrophic rat retinas: guanosine 3′,5′ cyclic monophosphate anomalies during photoreceptor cell degeneration. Exp. Eye Res. *20*, 585–597.

Lyubarsky, A.L., and Pugh, E.N., Jr. (1996). Recovery phase of the murine rod photoresponse reconstructed from electroretinographic recordings. J. Neurosci. *16*, 563–571.

Lyubarsky, A.L., Falsini, B., Pennesi, M.E., Valentini, P., and Pugh, E.N., Jr. (1999). UV- and midwave-sensitive cone-driven retinal responses of the mouse: a possible phenotype for coexpression of cone photopigments. J. Neurosci. *19*, 442–455.

Marszalek, J.R., Liu, X.R., Roberts, E.A., Chui, D., Marth, J.D., Williams, D.S., and Goldstein, L.S.B. (2000). Genetic evidence for selective transport of opsin and arrestin by kinesin-II in mammalian photoreceptors. Cell *102*, 175–187.

Nikonov, S., Lamb, T.D., and Pugh, E.N., Jr. (2000). The role of steady phosphodiesterase activity in the kinetics and sensitivity of the light-adapted salamander rod photoresponse. J. Gen. Physiol. *116*, 795–824.

Organisciak, D.T., Xie, A., Wang, H.-M., Jiang, Y.-L., Darrow, R.M., and Donoso, L.A. (1991). Adaptive changes in visual cell transduction protein levels: effect of light. Exp. Eye Res. *53*, 773–779.

Orr, H.T., Lowry, O.H., Cohen, A.I., and Ferrendelli, J.A. (1976). Distribution of 3′:5′-cyclic AMP and 3′:5′-cyclic GMP in rabbit retina in vivo: selective effects of dark and light adaptation and ischemia. Proc. Natl. Acad. Sci. USA *73*, 4442–4445.

Pennesi, M.E., Lyubarsky, A.L., and Pugh, E.N., Jr. (1998). Extreme responsiveness of the pupil of the dark-adapted mouse to steady retinal illumination. Invest. Ophthalmol. Vis. Sci. *39*, 2148–2156.

Philp, N.J., Chang, W., and Long, K. (1987). Light-stimulated protein movement in rod photoreceptor cells of the rat retina. FEBS Lett. *225*, 127–132.

Pugh, E.N., Jr., and Lamb, T.D. (2000). Phototransduction in vertebrate rods and cones: molecular mechanisms of amplification, recovery and light adaptation. In Handbook of Biological Physics. Molecular Mechanisms in Visual Transduction. Stavenga, D.G., De Grip, W.J., and Pugh, E.N., Jr., eds. (Amsterdam: Elsevier), pp. 183–255.

Pugh, E.N., Jr., Nikonov, S., and Lamb, T.D. (1999). Molecular mech-

anisms of vertebrate photoreceptor light adaptation. Curr. Opin. Neurobiol. *9*, 410–418.

Rodieck, R.W. (1998). The First Steps in Seeing. (Sunderland: Sinauer).

Roof, D.J., and Heth, C.A. (1988). Expression of transducin in retinal rod photoreceptor outer segments. Science *241*, 845–847.

Smith, N.P., and Lamb, T.D. (1997). The a-wave of the human electroretinogram recorded with a minimally invasive technique. Vision Res. *37*, 2943–2952.

Tai, A.W., Chuang, J.Z., Bode, C., Wolfrum, U., and Sung, C.H. (1999). Rhodopsin's carboxy-terminal cytoplasmic tail acts as a membrane receptor for cytoplasmic dynein by binding to the dynein light chain Tctex-1. Cell *97*, 877–887.

Tam, B.M., Moritz, O.L., Hurd, L.B., and Papermaster, D.S. (2000). Identification of an outer segment targeting signal in the COOH terminus of rhodopsin using transgenic *Xenopus laevis*. J. Cell Biol. *151*, 1369–1380.

Terakita, A., Takahama, H., Tamotsu, S., Suzuki, T., Hariyama, T., and Tsukahara, Y. (1996). Light-modulated subcellular localization of the α-subunit of GTP-binding protein Gq in crayfish photoreceptors. Vis. Neurosci. *13*, 539–547.

Terakita, A., Takahama, H., Hariyama, T., Suzuki, T., and Tsukahara, Y. (1998). Light-regulated localization of the β-subunit of Gq-type G-protein in the crayfish photoreceptors. J. Comp. Physiol. [A] *183*, 411–417.

Thomas, M.M., and Lamb, T.D. (1999). Light adaptation and dark adaptation of human rod photoreceptors measured from the *a*-wave of the electroretinogram. J. Physiol. *518*, 479–496.

Tsang, S.H., Burns, M.E., Calvert, P.D., Gouras, P., Baylor, D.A., Goff, S.P., and Arshavsky, V.Y. (1998). Role for the target enzyme in deactivation of photoreceptor G protein in vivo. Science *282*, 117–121.

Whelan, J.P., and McGinnis, J.F. (1988). Light-dependent subcellular movement of photoreceptor proteins. J. Neurosci. Res. *20*, 263–270.

Wyszecki, G., and Stiles, W.S. (1982). Color Science: Concepts and Methods, Quantitative Data and Formulae. (New York: John Wiley & Sons).